Available online at www.sciencedirect.com

ScienceDirect

Energy Procedia 148 (2018) 954–961

Energy Procedia

www.elsevier.com/locate/procedia

73rd Conference of the Italian Thermal Machines Engineering Association (ATI 2018), 12-14 September 2018, Pisa, Italy

CFD modeling of combustion of a natural gas Light-Duty Engine

G. Gianetti[a,*], L. Sforza[a], T. Lucchini[a], G. D'Errico[a], P. Soltic[b], J. Rojewski[b], G. Hardy[c]

[a]*Politecnico di Milano, Dip. di Energia, via Lambruschini 4, I-20156 Milan (Italy)*
[b]*Empa, Automotive Powertrain Technologies, Überland Str. 129, 8600 Dübendorf (Switzerland)*
[c]*FPT Industrial, Motorenforschung, Schlossgasse 2, 9320 Arbon (Switzerland)*

Abstract

A CFD methodology to model natural gas Light-Duty SI (Spark-Ignition) engines is here proposed. The ignition stage is modeled by means of a simplified Eulerian spherical kernel approach (deposition model). Then, the fully turbulent flame propagation is reproduced by the Coherent Flamelet Model (CFM), where turbulence effects are taken into account by considering the flame surface density evolution. The laminar to turbulent flame transition is managed by the CFM model and it is assumed to occur when the flame radius reaches a fraction of the integral length scale. This methodology was validated with experimental data of in-cylinder pressure and heat release rate at different loads and speeds.

Keywords: CFD; natural gas; CFM; OpenFOAM.

1. Introduction

Nowadays the development of engines is mainly focused on the reduction of pollutants, and in particular CO_2 emissions. There are different technologies which are able to achieve this scope, but most of them entail an increase of the system cost. One of the most effective solution, in particular for commercial vehicles, is to derive from a Diesel based engine a natural gas variant. The use of natural-gas as a fuel offers various advantages: first of all the high H/C ratio results in a decrease of CO_2 emissions with respect to other fuels and the use of a gaseous fuel reduces a lot the formation of particulate matter. Moreover, the opportunity to operate with lean mixture leads also to high thermal efficiency and low nitrogen oxides emissions.

Within this context, a detailed study of the combustion process is the only way to achieve more and more efficient solutions. The use of computational fluid dynamics (CFD) becomes a powerful and efficient tool since it allows to

*Corresponding author. Tel.: +39 02 2399 3909 ; fax: +39 02 2399 3913.
E-mail address: giovannigaetano.gianetti@polimi.it

10.1016/j.egypro.2018.08.067

investigate in detail all the processes (ignition, laminar and turbulent combustion) that take place inside the combustion chamber.

The most used turbulent combustion models are the assumed probability density function model (PDF) [1]-[2], the eddy breakup model (EBU) [3]-[4] and the coherent flamelet model (CFM) [5]-[6]. The PDF model solves transport equation for the fluctuation of the reaction progress or mixture fraction variable. Both EBU and the CFM model assume that the mean reaction rate is controlled by the turbulent mixing time. The advantage of the CFM model lies in the decoupled treatment of the turbulent flow and the chemical reaction, whereas the EBU model does not consider the chemical effects. Since the CFM model is based on the laminar flamelet concept [7], the flame surface density (FSD) equations are valid only when a fully established flame front is considered. Therefore a model for the ignition process is required and plays a fundamental role in the evolution of the whole combustion process, since it affects the ignition timing and the first development of the flame during the quasi-laminar phase.

In this work, a CFD methodology to model natural gas Light-Duty SI engines is proposed. The ignition is described by means of a deposition model and the flame surface density equation is solved according to the Choi and Huh formulation. Tabulated kinetics was included in the proposed approach to estimate the burned gas composition with the possibility, in future work, to employ it also for prediction of knock and the main pollutant emissions (CO, soot, NO_x). Fig. 1 summarizes the interaction between CFD solver, CFM model and look-up table: taking from CFD domain the main thermodynamic data, the CFM model computes the progress variable reaction rate, whereas the chemical composition of the burned gases is estimated by the look-up table. The proposed computational approach has been implemented inside the LibICE code, which is a set of libraries and solvers for internal combustion engine modeling based on the open-source OpenFOAM® technology.

The validation of the described models is performed on a natural gas Light-Duty SI engine at different operating conditions. A low load and two high loads operational points are tested at three different rotational speeds. Turbulence is described through a RANS approach by means of the $k-\epsilon$ model. Validation is carried out by a comparison between computed and experimental data of in-cylinder pressure, heat release rate and mass burning rate.

2. Numerical Models

The combustion process in a premixed spark-ignited engine is divided into three phases: ignition, laminar and turbulent propagation. Here are reported the different models used for modeling these phases.

2.1. Ignition modeling

In SI engine the combustion process is initiated by an electrical spark generated by the spark plug, which creates a initial flame kernel that propagates in an almost spherical way during the laminar phase. This phenomenon is modeled in this work by means of a deposition model, in which:

- The user defines an initial kernel diameter d_k, the spark plug location x_{spk} and a certain duration Δt_{spk}.
- In cells where the distance between the spark plug x_{spk} and the cell center is lower than the kernel radius $r_{spk} = d_{spk}/2$, a source term is applied for the specified duration Δt_{spk} to simulate ignition.
- The reaction rate during ignition $\dot{\omega}_{c,ign}$ is given by

$$\dot{\omega}_{c,ign} = (c_{max} - c_0)\frac{\rho_u}{\Delta t_{ignition}} C_S \tag{1}$$

where c is the progress variable, ρ_u is the unburnt gases density and C_S is a model constant.

Until the normalized progress variable does not reach a value c_{ign} close to 1 in the CFD domain, a quasi-laminar profile is imposed for the flame surface density distribution using the formula proposed by Weller [8]

$$\Sigma = |\nabla c| \tag{2}$$

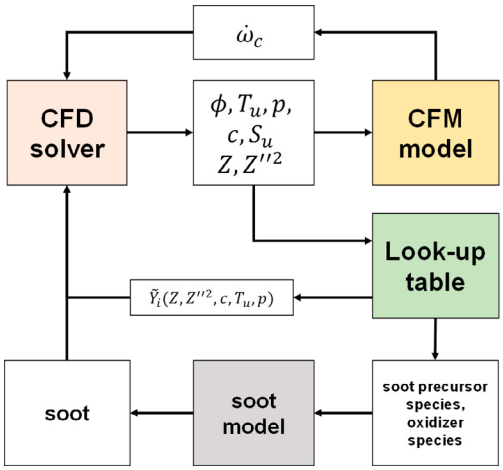

Fig. 1. Combustion model work flow.

During the quasi-laminar phase, the burning rate mainly depends on the ignition source. When the maximum progress variable reaches c_{ign} in one cell, the flame surface density equation is solved accordingly to the Choi and Huh formulation [9] described below.

2.2. Laminar and turbulent propagation modeling

The coherent flamelet model is based on the assumption of the laminar flamelet concept, in which the turbulent premixed flame is viewed as a collection of one-dimensional, planar laminar flamelets. The main advantage of the CFM model is the decoupled treatment of the chemical and turbulence effects. The mass burning rate per unit volume is given as

$$\dot{w} = \rho_u I_0 U_L \Sigma \tag{3}$$

where ρ_u is the fresh gas density, U_L the unstrained laminar burning velocity, Σ the flame surface density and I_0 is the mean stretch factor, function of the Markstein and Karlovits numbers [10]. Chemical and molecular effects are represented by the laminar burning velocity U_L, whereas the turbulence effects are represented by the flame surface density Σ. Then, a conservation equation for Σ is solved

$$\frac{\partial \Sigma}{\partial t} + \frac{\partial}{\partial x_i}(U_i \Sigma) = \frac{\partial}{\partial x_i}\left(\frac{\nu_t}{\sigma_\Sigma}\frac{\partial \Sigma}{\partial x_i}\right) + S - D \tag{4}$$

where ν_t is the turbulent kinematic viscosity, σ_Σ the turbulent Schmidt number, S and D are the production of flame surface by turbulent rate of strain and the annihilation of flame surface by mutual collision correspondingly.

The laminar and turbulent propagation phases are described in this model using the same flame surface density conservation equation but varying the source terms: during the laminar combustion, the production term is given by a weighted average with the proper limiting forms of purely laminar and fully turbulent growth and the annihilation term is omitted:

$$S = \alpha \left[\left(1 - \frac{R(t)}{l_t}\right) e_l + \frac{R(t)}{l_t} e_t\right] \Sigma \tag{5}$$

$$e_l = 2\left(\frac{\rho_u}{\rho_b}\right)\frac{U_L}{R(t)} \tag{6}$$

$$e_t = \frac{u'}{l_{tc}} \tag{7}$$

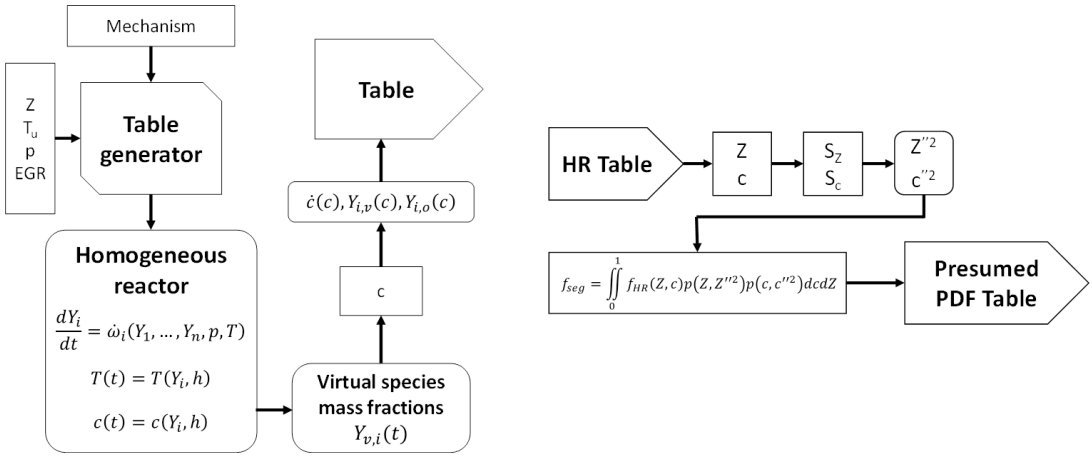

Fig. 2. Tabulated kinetics diagram.

$$R(t) = U_L(t - t_{ign})\frac{T_b}{T_u} + r_0 \tag{8}$$

where α and l_{tc} are two model constants, $R(t)$ is the flame radius, whose growth depends on the laminar burning velocity and the ratio between burnt and unburnt gases temperatures. On the other hand, the turbulent combustion source terms are:

$$S = \alpha\frac{u'}{l_{tc}}\Sigma \tag{9}$$

$$D = \beta\frac{U_L}{\left(\frac{\tilde{Y}}{Y_0}\right)\left(1 - \frac{\tilde{Y}}{Y_0}\right)}\Sigma^2 \tag{10}$$

where $\tilde{Y}$ is the mean fuel mass fraction, Y_0 the fuel mass fraction in the fresh mixture and β a model constant. D is given proportional to Σ^2 since annihilation occurs due to collision between flame surfaces.

The transition between laminar and turbulent propagation phase is assumed to occur when the flame radius $R(t)$ reaches a fraction of the integral length scale l_t. According to Cheng and Diringer [11] the fraction value is equal to 0.26.

2.3. Tabulated kinetics

Combined operation of the proposed combustion model and tabulated kinetics is reported in Fig. 2. The look-up table generator is mainly a Python program which exploits the Cantera library to perform auto-ignition simulations at constant pressure for different user-specified values of equivalence ratio and unburned gas temperature. Computed results are then processed and stored in a look-up table which includes both chemical composition and progress variable reaction rate. In this work, the progress variable reaction rate is computed with the CFM model and the look-up table is only used to estimate the chemical composition of the burned gases. Incorporation of tabulated kinetics reduces the computational time since no chemical equilibrium calculations are necessary to estimate the composition of the burned gases. Moreover, availability of reaction rates at homogeneous conditions will make possible to exploit tabulated kinetics also for prediction of knock or advanced combustion models (like spark-assisted compression ignition) in future works.

Table 1. Details of the simulated operating conditions.

Case name	A100	B25	C100
Engine speed [*rpm*]	1600	2000	3000
BMEP [*bar*]	11.5	4.3	9.6
Lambda [-]	1.00	1.00	1.00
EGR [%]	0.00	0.00	0.00
Spark Advance [*aTDC*]	-24.2	-18.3	-25.8

3. Validation

3.1. Case setup

The used models were tested on three different operating conditions of a 3.0L natural gas Light-Duty SI engine. The main engine data and simulated conditions are provided in Tab. 1. The operational points A100 and C100 are two full-load conditions, whereas the operational point B25 is a low load condition.

The geometry is a 2D representation of half of the engine combustion chamber. In order to have a good control on the cells shape and dimension, the mesh was generated using a block structured grid. Fig. 3 shows the mesh at the top dead center whereas Tab. 2 summarizes mesh main characteristics and engine dimensions. Mesh motion was performed using the dynamic mesh layering technique [12], keeping fixed the cells in the spark plug region and moving the ones in the piston bowl.

Simulations start at inlet valve closing (IVC) and the initial thermodynamics conditions were derived form experimental data. The in-cylinder velocity field and turbulence were initialized taking the swirl motion into account. A dedicated utility developed inside the LibICE library initializes:

- The radial component of the velocity field according to the swirl ratio provided by the user.
- The axial component of the velocity field according to the instantaneous piston velocity inside the piston bowl. Depending on the distance of the point from the cylinder head, the velocity linearly decreases from piston velocity to zero.

Furthermore, the utility also initializes the turbulent kinetic energy k and the rate of dissipation of turbulent energy ϵ according to the following formula:

$$k = \frac{3}{2}u'^2 = \frac{3}{2}(C_{up}\bar{u}_p)^2 \tag{11}$$

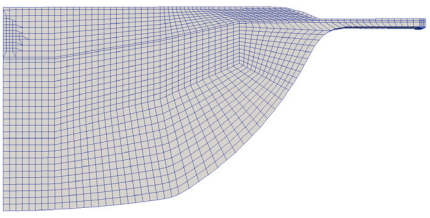

Fig. 3. 2D grid representing half of the combustion chamber.

$$\epsilon = \frac{C_\mu^{0.75} k^{1.5}}{L_i} = \frac{C_\mu^{0.75} k^{1.5}}{C_L \cdot D} \tag{12}$$

where $\bar{u}_p$ is the mean piston speed, D is the engine bore, C_{up} and C_L are specified by the user. Therefore, k is computed assuming that turbulence intensity u' is a fraction of the mean piston velocity, whereas ϵ is calculated assuming that the integral length scale L_i is a fraction of the engine bore.

Table 2. Mesh main characteristics and engine dimensions.

Characteristic	Value
Mean cell dimension [*mm*]	0.7
Cell dimension near spark-plug [*mm*]	0.35
Min number of cells [-]	≈1700
Max number of cells [-]	≈10700
Bore [*mm*]	95.8
Stroke [*mm*]	104

This method allows to initialize the velocity field and the turbulence in a consistent way, but depends mainly on the geometrical data and on the engine speed, without taking into consideration the engine load. This means that a low load point, where the intake flow is highly throttled, is initialized with the same turbulence and velocity field of a full load operating condition, which is not really true. In order to have a proper initialization of the velocity and turbulence, a full-cycle simulation of the exhaust and intake process would be more appropriate.

The ignition method used for the simulations is simplified and depends mainly on the ignition source. To this end, a tuning of the ignition model was required in order to choose the main ignition constants.

3.2. Ignition model tuning

The operational point named C100 was selected to tune the ignition constants since it is the one with more defined boundary conditions, turbulence intensity and flow field. A flame kernel with a diameter d_k of 8 *mm* was then selected with a deposition time $\Delta t_{ignition}$ of 2 *ms* and a strength coefficient C_S of 12.

Using these coefficients the computed in-cylinder pressure is in good agreement with the experimental data, as it can be noticed in Fig. 4(a). The pressure peak is well predicted in terms of amplitude whereas is slightly in advance with respect to the experiments. This behavior can be explained looking at the burnt mass fractions reported in Fig. 4(b): while the ignition timing is well predicted, the turbulent burning rate is overestimated with respect to experimental data, causing a faster burning with a consequent anticipation of the pressure peak.

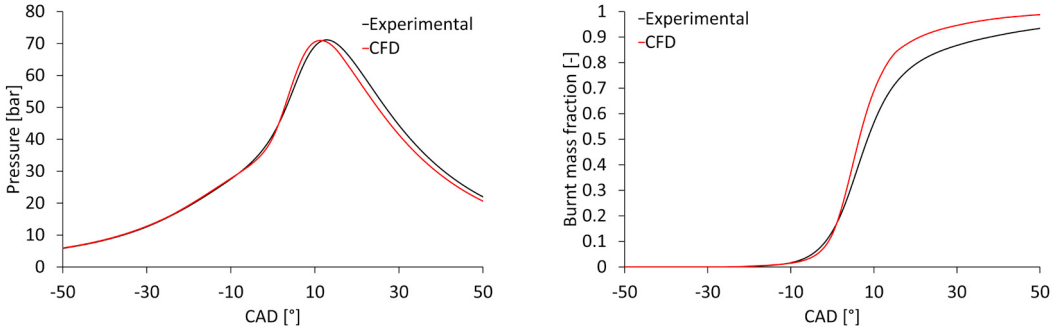

(a) *Pressure* (b) *Burnt mass fraction*

Fig. 4. Comparison between computed and experimental pressure for operating point C100 and burnt mass fraction.

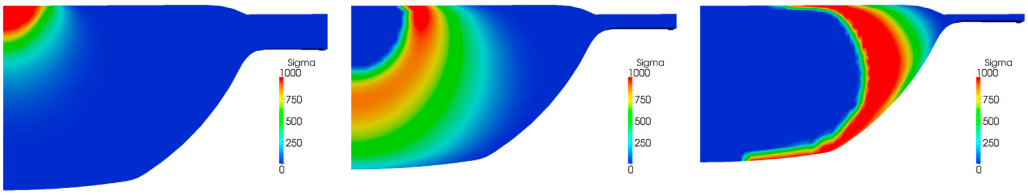

(a) *CAD: -20* (b) *CAD: -10* (c) *CAD: 0*

Fig. 5. Flame surface density evolution inside the combustion chamber.

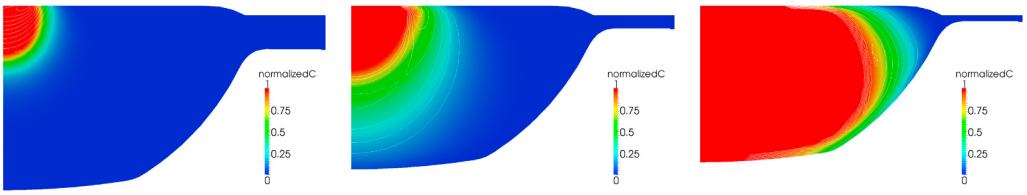

(a) *CAD: -20* (b) *CAD: -10* (c) *CAD: 0*

Fig. 6. Progress variable evolution inside the combustion chamber.

As it can be seen in Fig. 5 and Fig. 6, the flame surface density Σ and so the progress variable c evolve inside the combustion chamber as expected: at -20 CAD the flame is enclosed around the spark-plug. Then, it starts to evolve in an almost spherical way and burn the mixture as the piston moves towards the top dead center (TDC). Finally, the flame reaches correctly the liner and completes the burning of the mixture.

3.3. Validation on the other operational points

Using the same setup of the case C100, the other two operational points A100 and B25 were simulated. The full load point A100, Fig. 7(a), shows an underestimation of the pressure peak and a delay in the turbulent combustion development with respect to the experimental data. In the low load point B25 instead, Fig. 7(b), the switch between laminar and turbulent combustion occurs too early, and this entails an overestimation of the pressure peak which occurs in advance. This behavior may be related to the very low load condition (pressure is below 1 bar at IVC) and to poor air entrainment, but this aspect has to be further investigated.

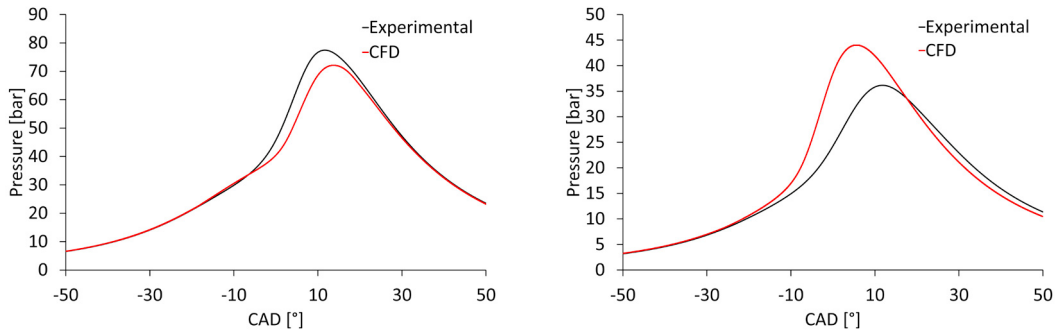

(a) *A100* (b) *B25*

Fig. 7. Comparison between computed and experimental pressure for operating point A100 and B25, using a flame kernel diameter of 8 *mm*.

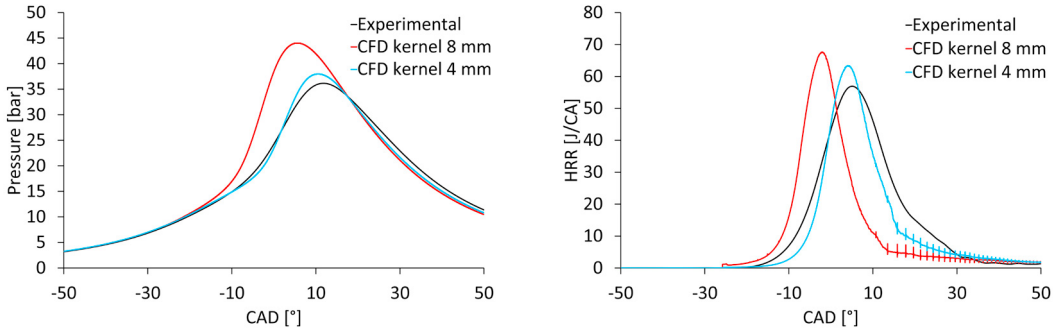

(a) *Pressure* (b) *Heat release rate*

Fig. 8. Comparison between computed and experimental pressure and HRR for operating point B25 using a flame kernel diameter of 4 *mm*.

In order to see the effects of the ignition model on the overall combustion process, the initial flame kernel diameter d_k was reduced from 8 *mm* to 4 *mm*. Fig. 8(a) shows the results of the new simulation. The overall pressure trend is improved with respect to the previous case, with a better estimation of the pressure peak position and amplitude, even if it is still slightly overestimated. Looking at the heat release rate in Fig. 8(b) it is possible to see that, using the smaller flame kernel, the HRR peak position is in good agreement with experimental data and also the amplitude is improved with respect to the previous case.

4. Conclusions

The purpose of this work was to show a CFD methodology to model natural gas Light-Duty SI engines. A simplified deposition model was used to describe the ignition of the mixture, whereas the turbulent flame propagation is reproduced by the CFM model.

The achieved results illustrate that the use of a simplified ignition model needs a proper tuning since it will affect the overall combustion process. Simulations on the full load operational points were in good agreement with the experimental pressure trace, the burnt mass fractions and the flame surface density evolved inside the combustion chamber as expected. The low load point B25 needed a later tuning since the results were not in agreement with experimental data. Some modifications to the ignition timings and ignition constants could be necessary since there is some uncertainties on turbulence quantities and swirl motion, but this particular aspect has to be further investigated.

References

[1] Bray KNC, Moss JB. “A unified statistical model of the premixed turbulent flame” *Acta Astronautica* 4:291 (1977).
[2] Borghi R, Argueyrolles B, Gauffie S, Souhaite P. “Twenty-First Symposium (International) on Combustion” *The Combustion Institute* p.1591 (1986).
[3] Spalding DB. “Thirteenth Symposium (International) on Combustion” *The Combustion Institute* p. 649 (1971).
[4] Magnussen BF, Hjertager BH. “Sixteenth Symposium (International) on Combustion” *The Combustion Institute* p. 719 (1977).
[5] Marble FE, Broadwell JE. “The Coherent Flamelet Model for Turbulent Chemical Reactions” *Project Squid* TRW-9-PU (1977).
[6] Maistret E, Darabiha N, Poinsot T, Veynante D, Lacas F, Candel S, Esposito E. “Numerical Combustion” *Springer-Verlag* p.98 (1989).
[7] Peters N. “Twenty-First Symposium (International) on Combustion” *The Combustion Institute* p. 1231 (1986).
[8] Weller HG. “The Development of a New Flame Area Combustion Model Using Conditional Averaging” *Thermo-Fluids Section Report* TF/9307 (1993).
[9] Choi CR, Huh KY. “Development of a Coherent Flamelet Model for a Spark-Ignited Turbulent Premixed Flame in a Closed Vessel” *Combustion and Flame 114* 336-348 (1998).
[10] Richard S, Colin O, Vermorel O, Benkenida A, Angelberger C, Veynante D. “Towards large eddy simulation of combustion in spark ignition engines” *Proceedings of the Combustion Institute 31* 3059-3066 (2007).
[11] Cheng WK, Diringer JA. “Numerical modelling of SI engine combustion with a flame sheet model” *SAE Paper* 910268 (1991).
[12] Lucchini T, D’Errico G, Jasak H, and Tukovic Z. “Automatic Mesh Motion with Topological Changes for Engine Simulation” *SAE Paper* 2007-01-0170 (2007).